J Appl Electrochem (2007) 37:1153–1162
DOI 10.1007/s10800-007-9379-0

ORIGINAL PAPER

Corrosion inhibition of aluminium in acid solutions by some imidazoline derivatives

M. A. Quraishi · M. Z. A. Rafiquee · Sadaf Khan · Nidhi Saxena

Received: 31 January 2007 / Revised: 5 July 2007 / Accepted: 13 July 2007 / Published online: 31 July 2007

Abstract 2-Pentadecyl-1,3-imidazoline (PDI), 2-Undecyl-1,3-imidazoline (UDI), 2-Heptadecyl-1,3-imidazoline (HDI), 2-Nonyl-1,3-imidazoline (NI) were synthesized and characterized by FT-IR and NMR Studies. The corrosion inhibition properties of these compounds on aluminium in 1 M HCl and 0.5 M H_2SO_4 were investigated by weight loss, potentiodynamic polarization, electrochemical impedance and scanning electron microscopic techniques. The weight loss study showed that the inhibition efficiency increases with increase in the concentration of the inhibitor and was found to be inversely related to time and temperature while it shows no significant change with increase in acid concentration. The effectiveness of these inhibitors were in the order of UDI > NI > PDI > HDI .The values of activation energy, free energy of adsorption, heat of adsorption, enthalpy of activation and entropy of activation were also calculated to elaborate the mechanism of corrosion inhibition. The adsorption of these compounds on aluminium surface follows the Langmuir adsorption isotherm. The potentiodynamic polarization data show that the compounds studied are mixed type inhibitors. Electrochemical impedance was used to investigate the mechanism of corrosion inhibition. The surface characteristics of inhibited and uninhibited metal samples were investigated by scanning electron microscopy (SEM).

M. A. Quraishi
Department of Applied Chemistry, Institute of Technology, Banaras Hindu University, Varanasi 221 005, India

M. Z. A. Rafiquee · S. Khan (✉) · N. Saxena
Corrosion Research Laboratory, Department of Applied Chemistry, Faculty of Engineering and Technology, Aligarh Muslim University, Aligarh 20 2002, India
e-mail: sadaf_khan5@rediffmail.com

Keywords Corrosion inhibitors · Aluminum · Scanning electron microscopy · Potentiodynamic polarization · Electrochemical impedance

1 Introduction

Aluminium has a great economic and industrial importance owing to its low cost, light weight and high thermal and electrical conductivity. An important feature of aluminium is its corrosion resistance due to the formation of a protective film on its surface upon exposure to the atmosphere or aqueous solutions [1–3]. Hydrochloric and sulphuric acid solutions are used for pickling of aluminium or for its chemical or electrochemical etching. It is very important to add a corrosion inhibitor to decrease the rate of aluminium dissolution in such solutions. The corrosion inhibition of aluminium in acid medium has been reported recently by using hydrazone [4], anionic surfactants [5] and amino acid [6] as inhibitors.

Imidazoline compounds are reported to show corrosion resistant behaviour on copper [7, 8] and mild steel [9]. However no substantial information is available on aluminium in acid medium by imidazoline derivatives as corrosion inhibitors. Thus, it was thought worthwhile to study the corrosion inhibition behaviour of newly synthesized imidazoline derivatives namely, 2-Nonyl-1,3-imidazoline (NI), 2-Undecyl-1,3-imidazoline (UDI), 2-Pentadecyl-1,3-imidazoline (PDI), 2-Heptadecyl-1,3-imidazoline (HDI) on aluminium in acidic medium. These compounds were derived from the respective fatty acids viz., capric, lauric, palmitic and stearic acid, with a view to establish their corrosion inhibition efficiencies along with the mechanism involved in their adsorption phenomenon.

2 Experimental details

Cold rolled aluminium strips of size 2 cm × 2.5 cm × 0.025 cm were used for weight loss measurements. For potentiodynamic polarization studies, aluminium strips coated with lacquer with an exposed area of 1 cm^2 were used. Electrodes were polished with emery papers of 1/0,2/0,3/0 and 4/0 grade and degreased with trichloroethylene. HCl and H_2SO_4 (MERCK) used for preparing solutions were of AR grade. Double distilled water was used to prepare solutions of 1 M HCl and 0.5 M H_2S0_4. The fatty acid imidazolines were synthesized as described by Hofmann [10] and the purity of the compounds was checked by TLC. The molecular structures and other details of these compounds are given in Table 1.

2.1 Synthesis of imidazoline derivatives

An appropriate amount of respective fatty acid (0.1 M) was dissolved in 50 ml absolute alcohol and treated with thionyl chloride (0.1 M). The mixture was refluxed for 3 h. The reaction product was then treated with ethylene diamine (6 ml) and was further refluxed for another 4 h. After the completion of the reaction, the solution was filtered, washed with water, dried and then crystallized in ethanol (Scheme 1).

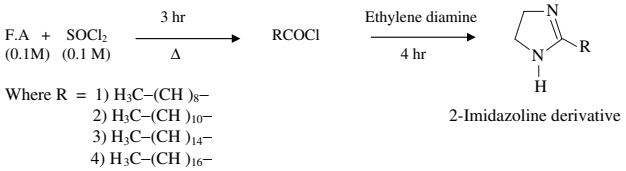

Scheme 1 Synthesis of imidazoline derivatives

2.2 FT-IR spectroscopy

FT-IR spectra of imidazoline derivative were obtained in KBr with Fourier transform spectrometer (Interspec 2020, UK), for the detection of various functional groups present in these inhibitors. FT-IR values are given in cm^{-1}.

2.3 NMR spectroscopy

^{1}H-NMR spectra run in $CDCl_3$ on a Bruker spectrospin 300 mHz spectrometer with TMS (Me_4Si) as the internal standard and its values are given in ppm (δ). The chemical shift was recorded relative to TMS assigned at zero. NMR helps in analyzing the type of protons attached to different groups of the inhibitors used.

Table 1 Name, structure and molecular weights of the compounds used

S.No	Structure	Name and abbreviation	Relative. mol. weight
1.	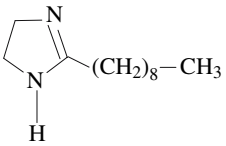	2-Nonyl-1,3-imidazoline (NI)	248
2	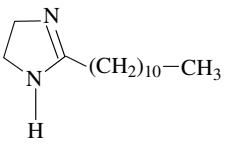	2-Undecyl-1,3-imidazoline (UDI)	276
3.	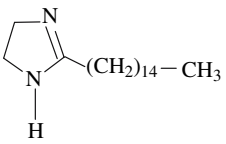	2-Pentadecyl-1,3-imidazoline (PDI)	332
4.	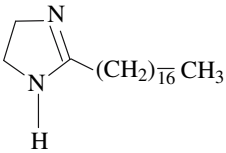	2-Heptadecyl-1,3-imidazoline (HDI)	360

2.4 Weight loss

A number of experiments were performed with varying concentrations of imidazoline derivatives for the weight loss of aluminium as per the ASTM method described previously [11]. The inhibition efficiency of these inhibitors was calculated using the following Equation:

$$IE = \frac{CR_o - CR_i}{CR_o} \times 100 \quad (1)$$

where

CR_o = Corrosion rate in blank hydrochloric and sulphuric acid

CR_i = Corrosion rate after adding inhibitors.

2.5 Potentiodynamic polarization

Potentiodynamic polarization studies were carried out using an EG and G Princeton Applied research (PAR) potentiostat/galvanostat (model 173), a universal programmer (model 175) and a X-Y recorder (model RE0089). A platinum foil was used as auxiliary electrode and a saturated calomel electrode (SCE) as reference for the potentiodynamic polarization studies. The CR was calculated using the equation [12],

$$CR = \frac{0.13 \times I_{corr} \times EW}{D} \quad (2)$$

where,

I_{corr} = Corrosion current density in μA cm^{-2}.

EW = Equivalent weight of the metal in gram.

D = Density of the metal in gcm^{-3}.

2.6 Electrochemical impedance studies

The electrical equivalent circuit for the system is shown in Fig. 1.

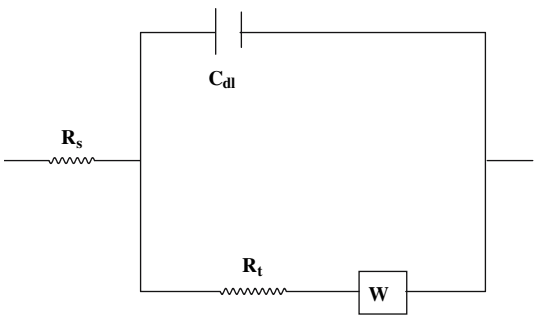

Fig. 1 Electrical equivalent circuit for the system (R_s = solution resistance, R_t = charge transfer resistance, C_{dl} = double layer capacitance, W = Warburg impedance)

The values of R_t and C_{dl} were obtained using Nyquist plots [13]. The %IE was calculated using the equation [14]:

$$IE\ \% = \frac{1/R_o - 1/R_t}{1/R_{to}} \times 100 \quad (3)$$

where R_t and R_{to} are the charge transfer resistance with and without inhibitor, respectively.

The impedance diagrams are not perfect semicircles and this difference has been attributed to frequency dispersion [15]. All the measurements were carried out using a Zahner IM-6 electrochemical workstation at 30 ± 2 °C, in the frequency range 5−100 kHz at E_{corr} for aluminium in 1 M HCl at different inhibitor concentration.

2.7 Scanning electron microscopy

A scanning electron microscope (SEM) [Model No 435 VP LEO] was used to study the morphology of the corroded surface in the presence and absence of inhibitors. The specimens were thoroughly washed with double distilled water before examination. To understand the morphology of the aluminium surface in the absence and presence of inhibitors, the following cases were examined.

(i) Polished aluminium specimen
(ii) Aluminium specimen dipped in 1 M HCl
(iii) Aluminium specimen dipped in 1 M HCl containing 500 ppm of UDI inhibitor.

3 Results and discussion

The structure elucidation was established by the results obtained from IR and NMR studies as under:

3.1 FT-IR spectroscopy

The FT-IR spectroscopic study was used to investigate the purity of the synthesized compound. The results are listed below:

(i) NI—IR (KBr): 1648 (C=N), 1352 (C–N), 2924 (C–H), 3146 (N–H), 1172 (CH_3) cm^{-1}.
(ii) UDI—IR (KBr) 1647 (C=N), 1323 (C–N), 2852 (C–H), 3257 (N–H), 1166 (CH_3) cm^{-1}.
(iii) PDI,—IR (KBr): 1640(C=N), 1463 (C–N), 2845 (C–H), 3290 (N–H), 1164 (CH_3) cm^{-1}.
(iv) HDI IR (KBr): 1665 (C=N), 1372 (C–N), 2845 (C–H), 2921 (N–H), 1250 (CH_3) cm^{-1}.

3.2 NMR spectroscopy

NMR spectral data ($\delta CDCl_3$)

UDI—7.350 (1H, NH), 1.936 (20H $(CH_2)_{10}$), 1.253 (3H, CH_3), 2.006 (4H, $(CH_2)_2$)

3.3 Weight loss

The imidazoline compounds inhibited corrosion rate of aluminium in both 1 M HCl and 0.5 M H_2S0_4 at all concentrations under study. Inhibition efficiency increases with increase in inhibitor concentration from 25 to 700 ppm (Figs. 2a and 3a). The maximum inhibition efficiency was achieved at 500 ppm and a further increase in inhibitor concentration caused no appreciable change in performance. The effect of immersion time on inhibition efficiency is shown in Figs. 2b and 3b. All the tested imidazoline show a decrease in inhibition efficiency with increase in immersion time from 2 to 24 h. This indicates de-sorption of the fatty acid imidazoline over a longer test period and may be attributed to various other factors such as increase in cathodic reaction or increase in ferrous ion concentration [16]. The influence of solution temperature on inhibition efficiency is shown in Figs. 2c and 3c. The inhibition efficiency for all the imidazolines decreases with increase in temperature from 30 to 60°C. The decrease in inhibition efficiency with rise in temperature may be attributed to desorption of inhibitor molecules at higher temperatures. From Figs. 2d and 3d, it is evident that increase in acid concentration from 1 to 3 M HCl and 0.5 to 1.5 M H_2SO_4 did not cause significant change in the e_{IE} values, thereby suggesting that all the compounds are effective corrosion inhibitors in acid solutions over this concentration range [17].

The degree of surface coverage (θ) for different inhibitor concentrations in 1 M HCl and 0.5 M H_2SO_4 at 30°C after 2-h immersion time was evaluated from weight loss values. The data were tested graphically by fitting to various isotherms. A plot of log (θ/1-θ) versus 1/T is shown in Figs. 4a and 5a. The heats of adsorption (Q) was calculated from the slope (−Q/2.303R) of the plot and are given in Table 2. The values of heat of adsorption (<−40 kJ mol^{-1}) suggest physical adsorption [18].

A number of authors [19–21] have reported that, in acid solution, the logarithm of the corrosion rate is a linear function of 1/T (Arrhenius equation):

$$\log\ (\text{Rate}) = \frac{-E_a^o}{2.303RT} + A \qquad (4)$$

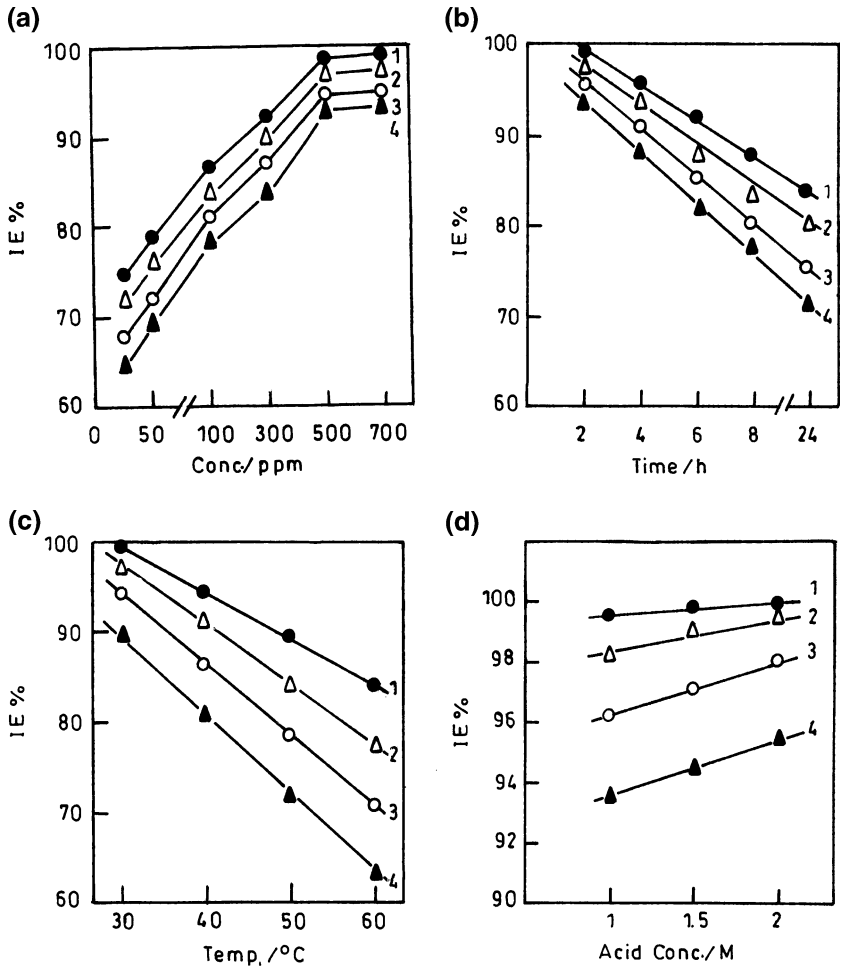

Fig. 2 Variation of inhibition efficiency with (**a**) inhibitor concentration, (**b**) immersion time, (**c**) solution temperature, (**d**) acid concentration in 1 M HCl (1: UDI; 2: NI; 3: PDI; 4: HDI)

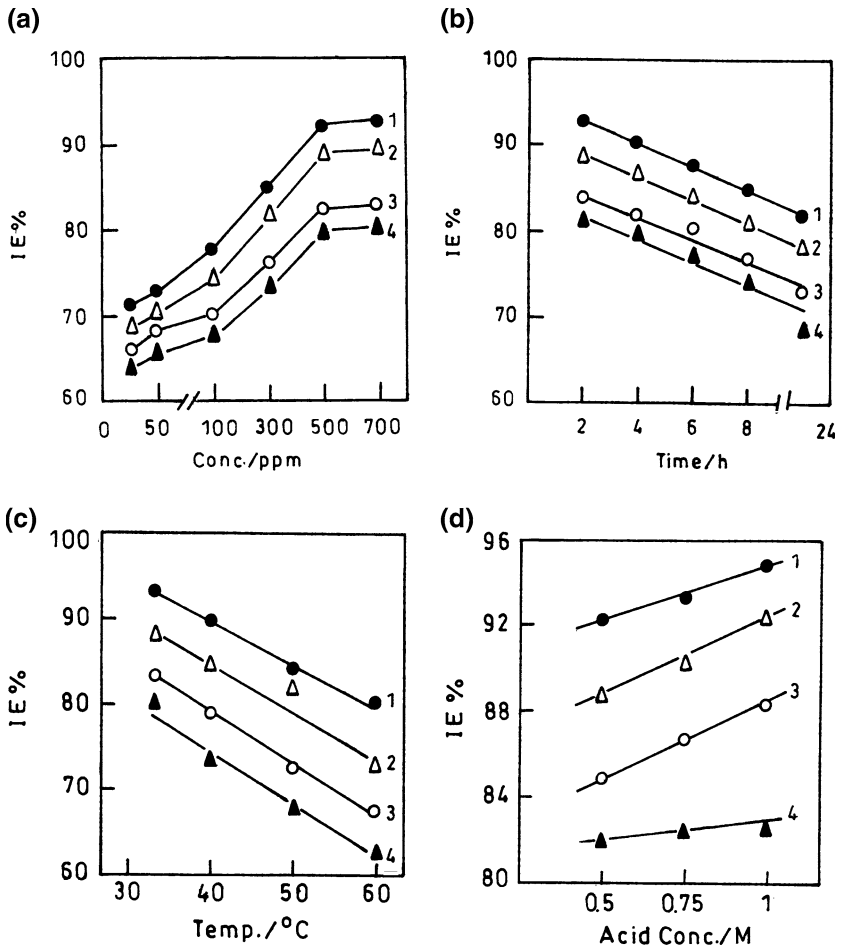

Fig. 3 Variation of inhibition efficiency with (**a**) inhibitor concentration, (**b**) immersion time, (**c**) solution temperature, (**d**) acid concentration in 0.5 M H_2SO_4 (1: UDI; 2: NI; 3: PDI; 4: HDI)

where, E_a^o is the apparent effective activation energy, R is the gas constant and A is the Arrhenius pre exponential factor. Plots of logarithm of corrosion rate obtained by weight loss measurement versus 1/T gave straight lines as shown in Figs. 4b and 5b.

The thermodynamic parameters (Table 2) show that the values of the activation energy $E_a^o$is higher for inhibited system as compared to the uninhibited system (Blank). The inhibition efficiency follows the order: UDI > NI > PDI > HDI. From the values of thermodynamic parameters, it is observed that the inhibitors are effective at lower temperatures [22].

An alternative formula for the Arrhenius equation is the transition state equation:

$$\text{Rate} = \frac{RT}{Nh}\exp\left(\frac{\Delta S^o}{R}\right)\exp\left(-\frac{\Delta H^o}{RT}\right) \quad (5)$$

where, h is the Plank constant, N is the Avogadro number, ΔS^o is standard entropy change and ΔH^o is the standard enthalpy change. A plot of log (CR/T) versus 1/T gave a straight line, (Figs. 4c and 5c) with a slope of $(-\Delta H^o/2.303 R)$ and an intercept of $[(\log (R/Nh) + (\Delta S^o/2.303 R)]$, from which the values of ΔS^o and ΔH^o were calculated. The values of standard enthalpy change, ΔH^o (Table 2) follow the order UDI > NI > PDI > HDI for various imidazoline inhibitors [22]. The entropy change, ΔS^o in the absence and presence of inhibitors is large and negative indicating that the activated complex in the rate determining step represents an association rather than a dissociation step. Thus a greater degree of orderliness appears during its transformation from reactant to activated complex [23].

The free energy of adsorption (ΔG_{ads}), was calculated by using the following equations [24] and the values are given in Table 2.

$$\Delta G_{ads} = - RT \ln (55.5 K) \quad (6)$$

where the equilibrium constant is

$$K = \theta / C (1 - \theta) \quad (7)$$

where θ is degree of coverage and C is inhibitor concentration in mol l^{-1}. The low and negative value of ΔG_{ads} indicate spontaneous physical adsorption [25].

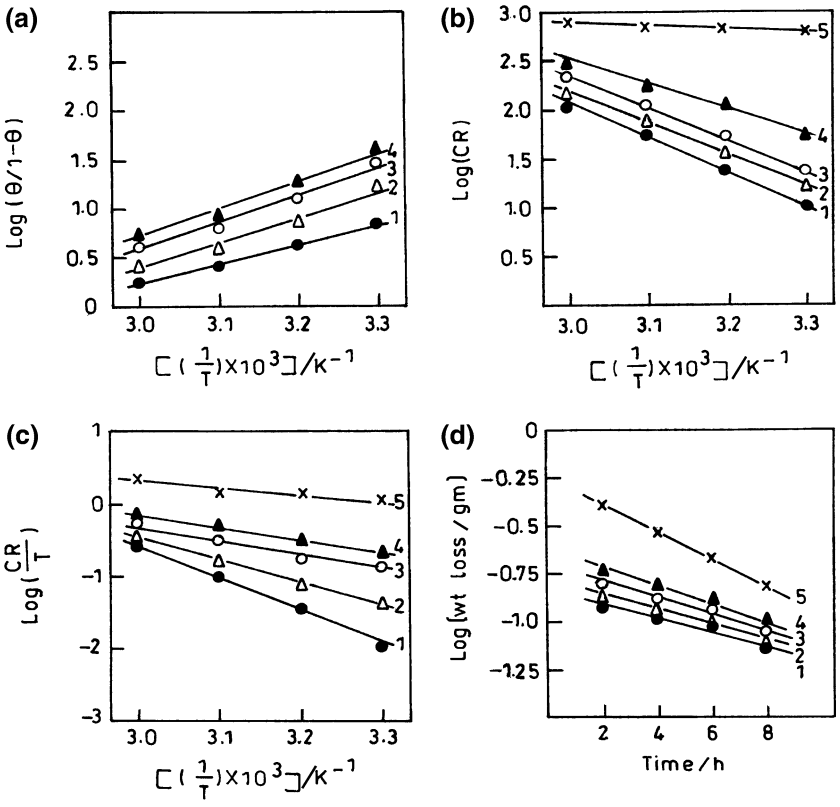

Fig. 4 Plots of (**a**) log ($\theta/1-\theta$) vs. 1/T; (**b**) log (CR) vs. 1/T; (**c**) log (CR/T) vs. 1/T; and (**d**) log (weight loss) versus immersion time in 1 M HCl (1: UDI; 2: NI; 3: PDI; 4: HDI; 5: Blank)

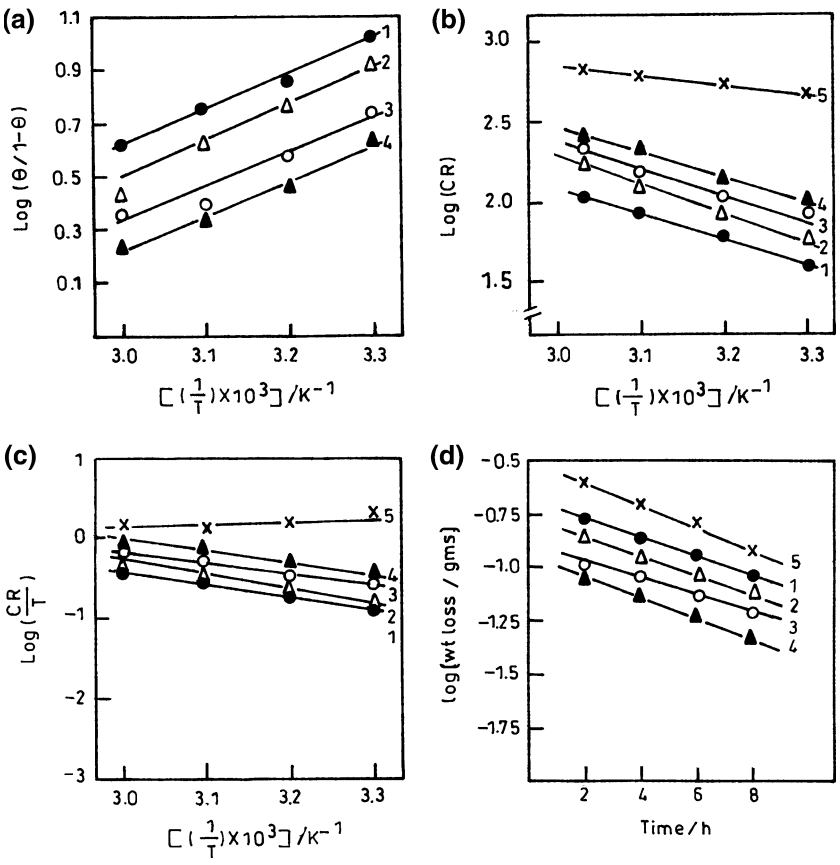

Fig. 5 Plots of (**a**) log ($\theta/1-\theta$) vs. 1/T; (**b**) log (CR) vs. 1/T; (**c**) log (CR/T) vs. 1/T; and (**d**) log (weight loss) vs. immersion time in 0.5 M H_2SO_4 (1: UDI; 2: NI; 3: PDI; 4: HDI; 5:Blank)

Table 2 Thermodynamic activation parameters for dissolution of aluminium in 1 M HCl and 0.5 M H_2SO_4 in absence and presence of 500-ppm inhibitor

System	E_a (kJ mol^{-1})	ΔH (kJ mol^{-1})	$-\Delta S$ (J $mol^{-1}K^{-1}$)	$-\Delta G_{ads}$ (kJ mol^{-1})	$-Q$ (kJ mol^{-1})
1 M HCl	9.57	22.34	189.94	–	–
UDI	67.02	76.58	210.70	35.18	38.29
NI	60.03	60.63	207.17	33.12	35.10
PDI	57.44	31.91	205.26	32.59	31.90
HDI	47.86	25.53	199.51	31.52	28.72
0.5 M H_2SO_4	12.76	9.57	194.7	–	–
UDI	25.53	31.91	207.17	32.32	26.17
NI	31.89	28.72	204.94	31.20	25.53
PDI	35.10	22.33	198.56	30.89	24.25
HDI	25.53	19.15	201.43	30.48	22.97

The rate of dissolution of metal in the presence and absence of inhibitors in acidic solution was studied by observing the weight loss at various times. The reaction was followed up to 90% of the dissolution of the metal. A straight-line plot (Figs. 4d and 5d) was obtained for log (weight loss) versus immersion time indicating that dissolution follows first order kinetics.

The values of the rate constant were calculated using the following first order rate law [26].

$$k = \frac{2.303}{t} \log \frac{[A_o]}{[A]} \quad (8)$$

where $[A_o]$ is the initial mass of the metal and [A] is the mass corresponding to time t. The half-life ($t_{1/2}$) value was calculated [27] using the following relationship:

$$t_{1/2} = 0.693/k \quad (9)$$

The values of rate constants and half-life periods obtained are summarized in Table 3. The value of rate constant (k) was found to be higher in the case of inhibited metal samples than few uninhibited samples. The corrosion rate is higher in the absence of inhibitors than with inhibited aluminium samples. Half-life values provide information regarding the rate of dissolution of coated and uncoated samples. The half-life periods in the presence of various inhibitors are in the order UDI > NI > PDI > HDI. The blank sample has the lowest $t_{1/2}$ value.

Table 3 The values of first order rate constant and half-life period for the dissolution of aluminium

System	10^{-2} k (h^{-1})	$t_{1/2}$ (h)
1 M HCl	18.690 ± 0.227	3.06
UDI	0.641 ± 0.089	108.11
NI	0.789 ± 0.104	87.84
PDI	1.660 ± 0.021	41.75
HDI	2.702 ± 0.038	25.64
0.5 M H_2SO_4	14.7 ± 0.184	4.71
UDI	1.156 ± 0.013	59.95
NI	1.659 ± 0.019	41.77
PDI	2.060 ± 0.024	33.64
HDI	2.370 ± 0.282	29.24

Reaction condition: [inhibitor] = 500 ppm, Temperature = 30 °C

3.4 Application of adsorption isotherm

The mechanism of corrosion inhibition may be explained on the basis of adsorption of imidazoline compounds [28]. The degrees of surface coverage (θ) for different inhibitor concentrations were evaluated from weight-loss data. Data were tested graphically by fitting to various isotherms. A plot of log $[\theta/(1-\theta)]$ vs. log C shows a straight line (Fig. 6a, b) indicating that adsorption in both the acids follows the Langmuir isotherm.

$$\theta/(1-\theta) = k\,C \exp(-G_{ads}/RT) \quad (10)$$

where G_{ads} is the free energy of adsorption and C is the inhibitor concentration.

3.5 Potentiodynamic polarization studies

The cathodic and anodic polarization curves of aluminium in 1 M HCl and 0.5 M H_2SO_4 in the absence and presence of different inhibitors at 500-ppm concentration at 28 ± 2°C are shown in (Fig. 7a and b). Electrochemical parameters such as corrosion current density (I_{corr}), corrosion potential (E_{corr}), Tafel constants, b_a and b_c, and % inhibition efficiency were calculated from Tafel plots and are given in Table 4. It is observed that the presence of inhibitor lowers I_{corr}. Maximum decrease in I_{corr} values was observed for UDI indicating that this is the most effective corrosion inhibitor among the studied imidazoline compounds, a trend obtained in conformity with weight loss data. It is also observed from Table 4 that E_{corr} values and Tafel slope constants b_a and b_c do not change

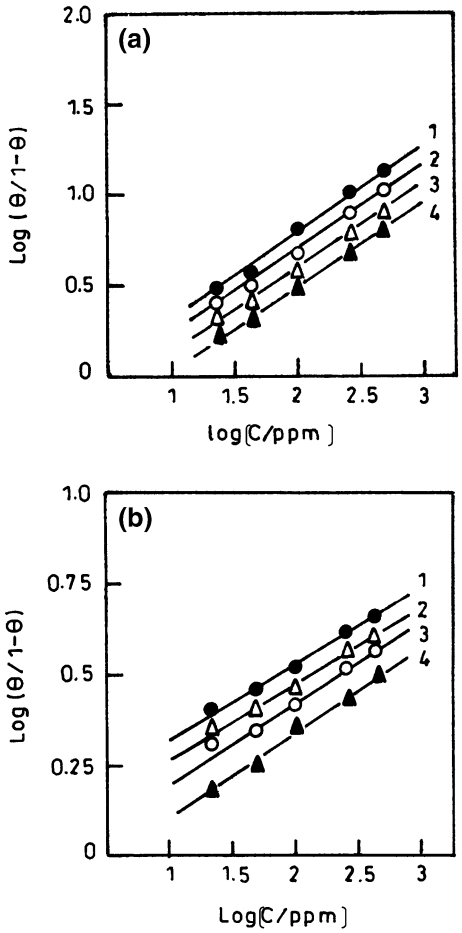

Fig. 6 Langmuir's adsorption isotherm plots for log $[\theta/(1-\theta)]$ versus log C for the adsorption of various inhibitors on the surface of aluminium in (**a**) 1 M HCl (**b**) 0.5M H_2SO_4 (1: UDI; 2: NI; 3: PDI; 4: HDI)

significantly in inhibited solution as compared to uninhibited solution. The imidazoline derivatives do not shift the E_{corr} values significantly, suggesting that they behave as mixed type inhibitors [29].

3.6 Electrochemical impedance study

The Impedance diagram obtained for aluminium in 1 M HCl is shown in Fig. 8 and the values of R_t, $C_{dl}$and %IE are given in Table 5. Values of R_t increases with increase in inhibitor concentration and this is, in turn, leads to an increase in the I.E [30]. A decrease in C_{dl} was observed with addition of 1 M HCl, suggesting that inhibition can be attributed to surface adsorption [31].

3.7 Scanning electron microscopy

Scanning electron microscopy of the metal samples of inhibited and uninhibited metal samples is presented in Fig. 9. The SEM study shows that the inhibited metal surface is found smoother than the uninhibited surface.

3.8 Mechanism of corrosion inhibition

In acidic solutions imidazoline compounds exist in protonated form. These protonated species are adsorbed on the cathodic sites through the π-electrons and lone pair electrons of nitrogen atoms of the imidazoline ring [28]. The observed order of e_{IE} (UDI > NI > PDI > HDI) can be explained on the basis of the nature of binding of the imidazoline ring to the metal surface and the length of the alkyl chain.

The binding of the imidazole ring to the metal surface can be presented by the diagram of Fig. 10. With the increase in chain length of the alkyl group (i.e. molecular weight), the number of imidazoline rings decreases in 500 ppm inhibitor concentration and therefore, e_{IE} decreases. The decrease in e_{IE} of NI may be due to its being least hydrophobic among the tested imidazolines and having less tendency to adsorb.

Therefore, UDI having (C_{11}) in its alkyl group has the highest adsorption to the metal surface. However the lower adsorption of PDI (C_{15}) and HDI (C_{17}) seems to be due to steric hindrance posed by the bulky alkyl groups in their adsorption phenomenon [32].

4 Conclusions

(1) The fatty acid imidazolines showed very good corrosion inhibiting behaviour for aluminium in both 1 M HCl and 0.5 M H_2SO_4 and follow the order UDI> NI > PDI > HDI.
(2) In weight loss studies, the e_{IE} of all imidazoline derivatives increase with increases in inhibitor concentration, whereas it decreases with increase in immersion time and temperature and shows no significant change with increase in acid concentration.
(3) Inhibition of aluminium surfaces in acid solutions is characterized by an adsorption mechanism which follows the Langmuir isotherm.
(4) All the compound studied behave as mixed-type inhibitors in both 1 M HCl and 0.5 M H_2SO_4.
(5) The Electrochemical study shows that the application of UDI, NI, PDI, HDI as inhibitors significantly increases R_t values and decreases C_{dl} values in 1 M HCl, suggesting that corrosion inhibition takes place by adsorption.
(6) Scanning Electron Microscopy shows a smoother surface for inhibited metal samples than uninhibited samples due to the formation of film like deposits on the inhibited surfaces.

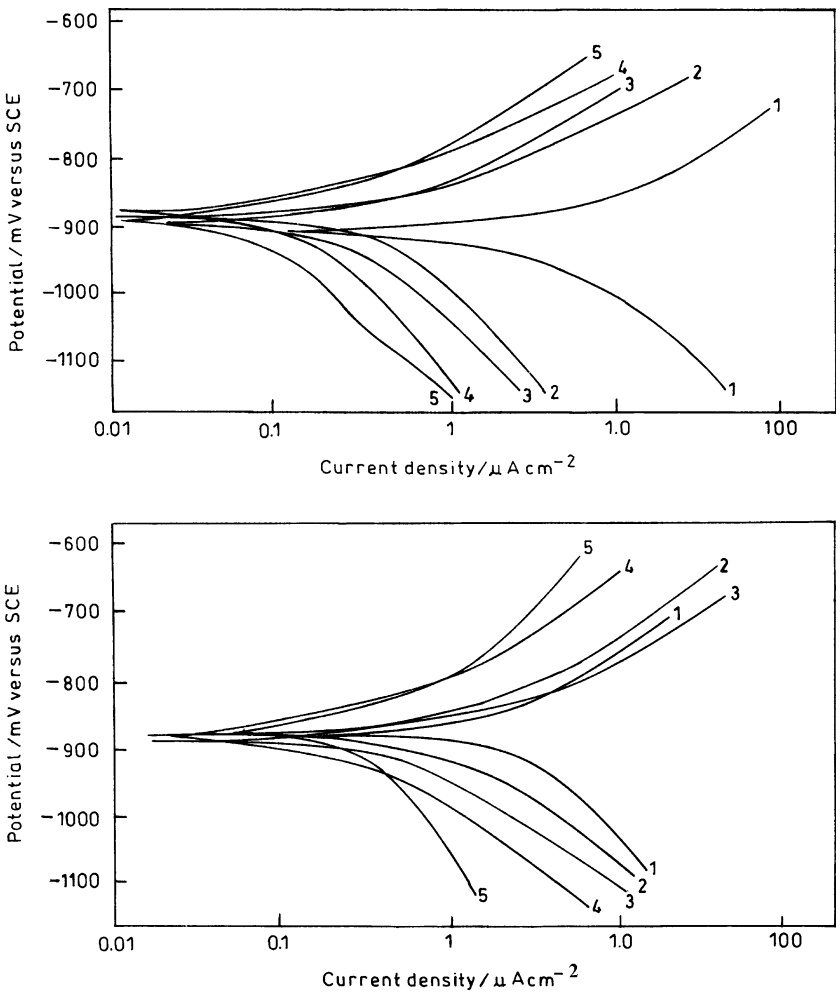

Fig. 7 Potentiodynamic polarization curves for aluminium containing 500-ppm imidazolines in (**a**) 1 M HCl (**b**) 0.5 M H_2SO_4 (1: Blank; 2: HDI; 3: PDI; 4: NI; 5: UDI)

Table 4 Electrochemical polarization parameters for the corrosion of aluminium in 1 M HCl and 0.5 M H_2SO_4 containing 500-ppm inhibitors at 30 °C

System	E_{corr}(mV)	I_{corr} (mA cm^{-2})	e_{IE} (%)	b_a (mV dec^{-1})	b_c (mV dec^{-1})
1 M HCl					
Blank	−902	4.490	–	68	174
UDI 500	−898	0.089	98.02	60	170
NI 500	−893	0.106	97.63	54	126
PDI 500	−890	0.184	93.91	56	114
HDI 500	−888	0.303	93.25	50	100
0.5 M H_2SO_4					
Blank	−890	4.160	–	56	120
UDI 500	−884	0.320	92.30	50	84
NI 500	−879	0.479	88.47	40	110
PDI 500	−880	0.681	83.63	54	94
HDI 500	−875	0.826	80.15	54	134

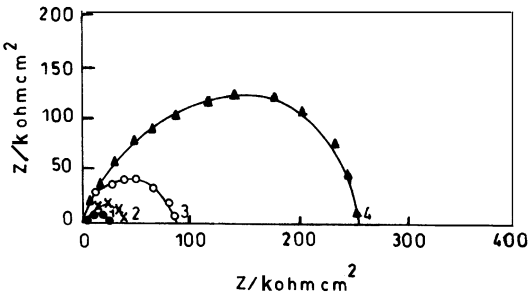

Fig. 8 Electrochemical impedance diagram (Nyquist plot) for aluminium in 1 M HCl in the absence and presence of UDI at different concentrations (1:Blank; 2: 25 ppm; 3: 100 ppm; 4: 500 ppm)

Table 5 Electrochemical impedance parameters for the corrosion of aluminium in 1 M HCl containing different concentrations of UDI at 30 °C

System	R_t (kΩ cm^2)	C_{dl} (F cm^{-2})	e_{IE} (%)
1 M HCl	16.23	4.51	–
UDI			
25	18.36	3.52	70.19
100	93.65	0.74	82.67
500	247.03	0.29	93.43

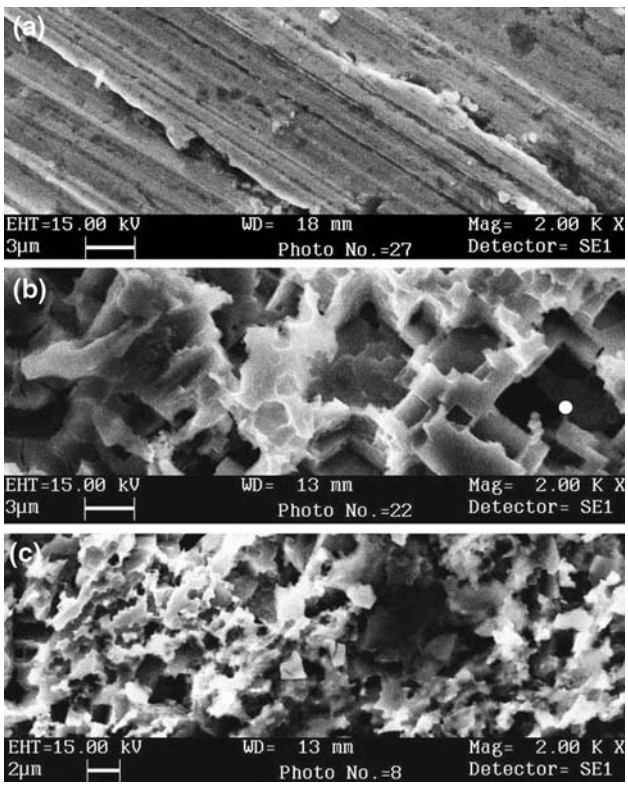

Fig. 9 Scanning electron micrographs of Polished aluminium (**b**) After dipping aluminium in 1 M HCl for 2 h (**c**) After dipping aluminium in 1 M HCl for 2 h containing 500 ppm UDI

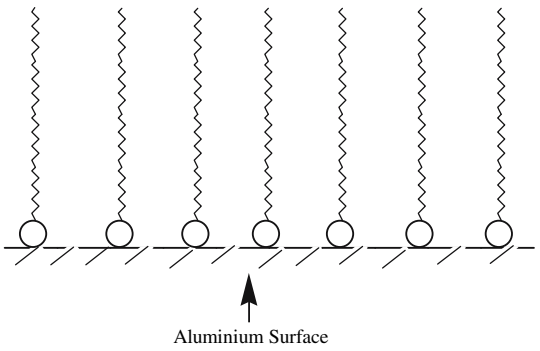

Fig. 10 Diagram showing corrosion inhibition of aluminium by imidazolines

References

1. Brett CM (1992) Corros Sci 33:203
2. Beck TR (1998) Electrochim Acta 33:1321
3. Hunkeler F, Frankel GS, Bohni H (1987) Corrosion 43:189
4. Ahmed Awad I, El-Asklany AH, Fouda AS (1985) J Indian Chem Soc 22:367
5. Tianpei Z, Guannan M (1999) Corros Sci 41:1937
6. Fouda AS, El-Semongy MM (1982) J Ind Chem Soc 19:89
7. Gasparac R, Martin CR, Stupnisek-Lisac E (2000) J Electrochem Soc 147:548
8. Zhang DQ, Gao LX, Zhu GD (2004) Corros Sci 46:3031
9. Muralidharan S, Iyer SVK (1997) Anti Corros Met Mat 44:100
10. Hoffmann K (1953) Imidazole and its derivatives –Part-I. The chemistry of heterocyclic compounds, Interscience publishers, Inc., New York, p 213
11. ASTM (1994) Standard practice for calculation of corrosion rate and related information from electrochemical measurements, annual book of standards, G 102-89
12. Schmidt G (1984) Br Corros J 19:99
13. Hirozawa ST (1995) Proc. 8th Eur. Symp Corros Inhi Ann Univ, Ferrara, Italy, 1:25
14. Ashassi-Sorkhabi H, Shaabani B, Seifzadeh D, (2005) Electrochim Acta 50:3446
15. Juttner K (1990) Electrochim Acta 35:1501
16. Quraishi MA, Rawat J (2001) Corrosion 19:273
17. Quraishi MA, Sardar R (2001) Corrosion 58:103
18. Jha LJ (1990) Studies of the adsorption of amide derivative during acid corrosion of pure iron & its characterization, PhD thesis, University of Delhi, p 111
19. Breslin CB, Carrol WM (1993) Corros Sci 34:327
20. Khedr MGA, Lashien MS (1992) Corros Sci 33:137
21. Rehim SSA, Hassan HH, Amin MA (2001) Mater Chem Phys 70:64
22. Putilova IN, Balezin SA, Baranik UP (1960) Metallic corrosion inhibitors. Pergamon Press, New York, p 31
23. Gomma MK, Wahdan MH (1995) Mater Chem Phys 39:209
24. Schorr M, Yahalom J (1972) Corros Sci 12:867
25. Gomma GK, Wahdan MH (1995) Ind J Chem Technol 2:107
26. Orubite-Okorosaye K, Oforka NC (2004), J Appl Sci Environ 8:57
27. Atkins PW (1980) Chemisorbed and physisorbed species, a textbook of physical chemistry. University press, Oxford, p 936
28. Quraishi MA, Mideen AS, Khan MAW, Ajmal M (1994) Ind J Chem Tech 1:329
29. Ajmal M, Mideen AS, Quraishi MA (1994) Corros Sci 36:79
30. Houyi M, Chen S, Yin B, Zhao S, Liu X (2003) Corros Sci 45:867
31. Subramaniyam NC, Mayanna S (1985) Corros Sci 25:163
32. Quraishi MA, Jamal D, Saxena N (2005) Ind J Chem Tech.12:225